REVIEW ARTICLE

Focused Ultrasound Combined with Microbubbles for Inducing Blood-Brain Barrier Opening: Cavitation Monitoring and Control

Na Li[a], *Fan Li*[b,*]

[a] *School of Health Science and Engineering, University of Shanghai for Science and Technology, Shanghai, China;* [b] *Department of Ultrasound, Shanghai Chest Hospital, Shanghai Jiao Tong University School of Medicine, Shanghai, China*

Received June 6, 2025; revision requested June 24, 2025; accepted October 14, 2025

Abstract: Focused ultrasound (FUS) represents an emerging non-invasive technique capable of achieving reversible and targeted opening of the blood-brain barrier (BBB) when combined with microbubbles (MBs), significantly enhancing drug permeability. This technology demonstrates considerable potential in preclinical studies for diagnosing and treating neurological disorders. Ensuring safe and effective BBB opening while preventing tissue injuries such as red blood cell extravasation remains a critical translational challenge. This review examines the mechanisms of FUS combined with MBs induced BBB opening, key influencing factors, and recent advances in strategies for monitoring and controlling in vivo cavitation activity, providing foundational insights for future research.

Key words: Focused ultrasound; Microbubbles; Blood-brain barrier; Control; Cavitation; Monitoring

Advanced Ultrasound in Diagnosis and Therapy 2026; 01: 001-008 DOI: 10.26599/AUDT.2026.250050

The blood-brain barrier (BBB) comprises brain microvascular endothelial cells, astrocyte end-feet, pericytes, tight junctions, and a basement membrane (diameter 4-8 μm) [1]. Its selective permeability maintains central nervous system (CNS) homeostasis but impedes trans-barrier transport for 98% of small molecules and nearly all large molecules [2,3], posing significant challenges for CNS therapeutics. Current BBB traversal strategies include invasive techniques such as intracranial injection and convection-enhanced delivery, which achieve high local drug concentrations but carry surgical risks [4,5]. Non-invasive approaches involving viral vectors and nanoparticle modifications frequently suffer from poor targeting and low delivery efficiency [6,7].

Focused ultrasound combined with microbubbles (FUS-MBs) technology has emerged as a promising solution due to its non-invasive nature, reversibility, and spatial precision. Optimized parameter combinations enable temporary BBB opening (recovery within 6-24 hours), with MRI-guided localization enhancing treatment accuracy. This approach has successfully delivered chemotherapeutic agents, antibodies, and nucleic acids [8-11] and shown potential for clearing β-amyloid plaques in Alzheimer's models [12,13]. Mechanistically, FUS exerts biological effects through thermal mechanisms (tumor ablation), mechanical forces (neuromodulation), and cavitation (primary BBB opening mechanism) [14]. Cavitation-generated mechanical stress during stable (SC) or inertial cavitation (IC) loosens endothelial tight junctions [15,16]. Despite advantages including non-invasiveness, deep-brain targeting, and scalable treatment areas, parameter misoptimization risks inflammation and hemorrhage [17]. Thus, elucidating mechanisms, refining parameters, and developing safety monitoring protocols are essential for clinical

[*] *Corresponding author: Department of Ultrasound, Shanghai Chest Hospital, Shanghai Jiao Tong University School of Medicine, 241 West Huaihai Road, Shanghai, 200030, China (Fan Li).*
e-mail: medicineli@sjtu.edu.cn (F L)

translation.

FUS-MBs Induced BBB Opening

Mechanisms

FUS-MBs-induced BBB opening involves synergistic physical and biological interactions (Fig. 1). FUS achieves sub-millimeter spatial focusing (diameter 1-2 mm, depth 8-15 mm), concentrating > 95% of acoustic energy non-invasively within target regions [18]. MBs (1-10 μm) serve as cavitation nuclei and drug carriers, amplifying energy conversion efficiency to enable BBB opening at low intensities (0.125-3 W/cm^2).

Cavitation is widely recognized as the primary mechanism [19], quantified by the mechanical index (MI = PNP/$\sqrt{f}$) [20]. At MI = 0.1-0.5, intravenously administered MBs undergo SC. Oscillating MBs displace adjacent endothelial cells during expansion and generate invaginations during contraction. Associated microjets and shear waves stretch cell membranes, widening tight junctions reversibly. At MI > 0.5, IC occurs. MBs collapse violently, producing mechanical stress, microjets, and localized hyperthermia that create endothelial micropores. While expanding BBB opening, IC increases vascular rupture risk [21-23]. Critically, SC drives reversible opening, whereas IC minimally contributes and correlates with tissue damage [15,16,24].

Acoustic radiation force enhances cavitation by aggregating MBs along wave propagation paths, increasing endothelial contact. Force magnitude depends on ultrasound intensity, frequency, and MB characteristics, enabling modulation of BBB opening. Two-photon microscopy reveals that MB expansion transiently reduces local blood flow. This ischemic effect may synergize with cavitation by activating endothelial hypoxia pathways [25,26]. The spatial selectivity of FUS-MBs ensures that only sonicated MBs near endothelia mediate localized BBB disruption [27].

At the molecular level, FUS-MBs upregulate caveolin-1 expression to promote transcytosis while activating Rho kinase and PI3K/AKT pathways. This cascade induces occludin phosphorylation and cytoskeletal reorganization, disassembling tight junction complexes [28]. This multifaceted synergy enables spatiotemporally controlled BBB opening for precision drug delivery.

Key factors influencing BBB opening safety and efficiency

Skull Skull acoustics critically constrain ultrasound transmission. Bone-soft tissue acoustic impedance mismatches and skull absorption and porosity cause amplitude attenuation and phase distortion [29]. Focal pressure decreases by 0.357 dB per 1 mm increase in skull thickness and 0.048 dB per 1 mm increase in transducer-skull distance. Interspecies skull thickness and density

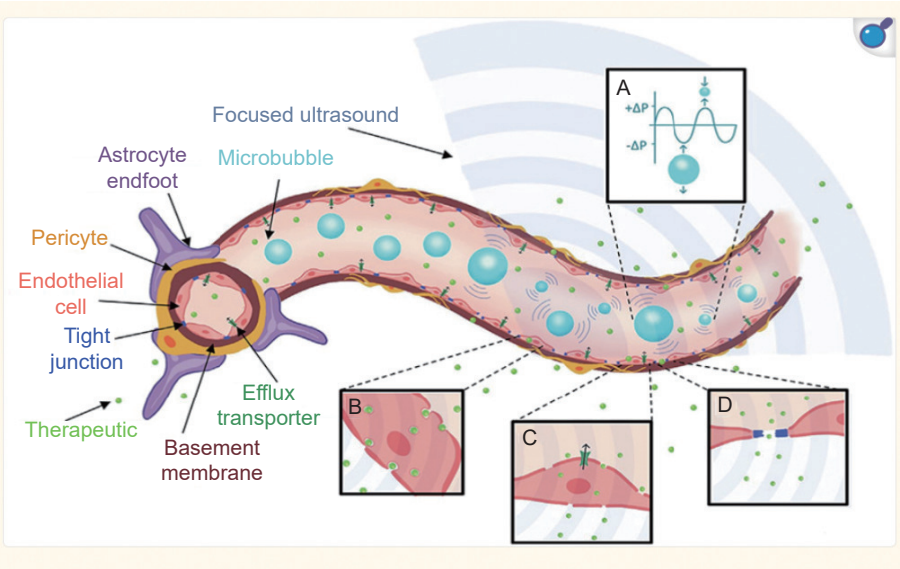

Qpen in a new tab

The physiology of the blood brain barrier, and the permeabilization of the blood brain barrier with microbubbles and focused ultrasound. (A) Focused ultrasound induced volumetric oscillations of microbubbles. (B) Transcytosis of a therapeutic through an endothelial cell. (C) Sonoporation of an endothelial cell. (D) Disruption of tight junctions between adjacent endothelial cells.

Figure 1 Schematic of BBB physiology and FUS-MBs mediated opening technology [15].

variations further modulate attenuation (e.g., positive correlation with rat body weight [30]). Notably, temporal and frontal bones exhibit higher transmission efficiency than occipital regions due to reduced thickness and favorable incidence angles [31]. Multi-element phased arrays improve beam focusing, while implantable ultrasound devices overcome attenuation in clinical glioblastoma trials [32]. Species-specific acoustic databases will facilitate parameter optimization.

Acoustic Parameters Frequency selection balances penetration depth and focusing precision. The 200 kHz-1.5 MHz range is optimal for transcranial applications, with 1.5 MHz considered a safe upper limit to minimize thermal injury [33]. Peak negative pressure (PNP) directly governs opening extent. Safe opening occurs at 0.3 MPa, while > 0.6 MPa risks tissue damage. A 10 ms pulse duration achieves optimal opening; longer durations (e.g., 100 ms) increase hemorrhage risk without efficacy gains, likely due to MB destruction. Duty cycles >10% may increase injury risk. Shorter burst lengths elevate PNP thresholds. Pulse repetition frequency (PRF) exerts dual effects. Higher PRF increases total pulses within fixed durations, enhancing opening extent. Lower PRF improves spatial uniformity [34,35]. Consequently, 1 Hz PRF is standard in preclinical and clinical studies [31].

Notably, a distinct saturation phenomenon exists in BBB opening: once a certain opening threshold is reached, further increasing acoustic parameters fails to enhance opening but instead elevates safety risks. This underscores the need for precise optimization of parameter combinations in practical applications to achieve safe and effective BBB opening.

Microbubbles Dynamics MBs physicochemical properties critically influence opening efficacy. Shell composition dictates biological effects. Optison® (albumin shell) exhibits superior opening capability and lower inflammation versus Definity® (lipid shell). A clear dose threshold exists. The clinical dose (10 μL/kg) causes mild inflammation, whereas 100 μL/kg activates inflammatory pathways [36]. Size effects are pronounced. MBs sized 1-2 μm permit BBB recovery within 24 hours. Those > 4 μm require 2-6 days. Larger MBs (6-8 μm) open BBB at lower pressures (0.15-0.30 MPa) than smaller MBs (0.30-0.46 MPa), reflecting mechanical constraints in capillaries [16]. Sterile inflammation is reduced with 1 μm versus 3-5 μm MBs at equal dosing [37]. These findings guide clinical MB selection.

Other Factors BBB opening area does not correlate with recovery time. Multitarget sonication increases the opening area 3.5-fold without prolonging repair [38]. Vessel size influences efficacy. The IC threshold is lower in venules/arterioles than capillaries, potentially due to greater mechanical confinement in small vessels [39]. Regional heterogeneity exists. The thalamus shows higher ultrasound sensitivity than the hippocampus under identical parameters, possibly reflecting vascular density differences [39]. MB injection rate, sonication delay, and target selection further modulate efficacy. Comprehensive device optimization, species-specific databases, and safety threshold definitions are vital for clinical translation.

Safety Monitoring and Control of FUS-MBs Induced BBB Opening

Monitoring cavitation activity

FUS-MBs induced BBB opening relies on cavitation effects, the safety of which is regulated by the interplay of acoustic parameters, MBs properties, and tissue heterogeneity. Factors such as individual variations in skull acoustics and regional vascular distribution affect local ultrasound energy deposition, while dynamic MB distribution in blood flow can cause abnormal local concentrations. These factors collectively contribute to spatiotemporal variability in cavitation effects and associated risks. Therefore, real-time monitoring of cavitation status and dynamic adjustment of ultrasound parameters based on this feedback are crucial for precise control of the BBB opening process.

The acoustic response characteristics of MBs provide a critical basis for real-time control of FUS-induced BBB opening. Research shows that MB acoustic response exhibits distinct pressure-dependent features. At pressures below 0.1 MPa, fundamental frequency scattering (f_0) predominates. As pressure increases, MB oscillation enters a weakly nonlinear phase, generating integer harmonics (e.g., 2 f_0, 3 f_0), indicative of SC. Further pressure increase into the strongly nonlinear phase leads to the emergence of ultraharmonics (e.g., 1.5 f_0, 2.5 f_0), signaling the transition towards IC. At pressures exceeding 1.5 MPa, MBs undergo violent expansion and collapse, generating broadband noise, a hallmark of IC and potential tissue damage [40,41]. Passive cavitation detection (PCD) systems quantify energy distribution across different frequency bands via spectral analysis, where harmonics/subharmonics correspond to stable cavitation intensity, and broadband noise reflects IC levels. This signal analysis method based on fast Fourier transform provides a reliable basis for real-time discrimination of cavitation type [42].

Controlling cavitation activity

Open-Loop Control Strategies Control strategies for cavitation activity have evolved from open-loop to

closed-loop approaches. In 2012, O'Reilly's team [43] pioneered feedback control based on ultraharmonic signals: upon detecting the target signal, the system automatically reduced acoustic pressure to 50% of the preset value. This method achieved over 95% detection accuracy, but transcranial signal attenuation limited its clinical application. In 2016, Tsai et al. [44] employed subharmonic energy spectral density monitoring combined with a confocal dual-frequency transducer system. Irradiation was terminated when the energy spectral density increased by 5.5 dB, achieving 92% sensitivity and 92.3% specificity for BBB opening monitoring in rats. Huang et al. [45] established a human skull-pig brain composite model and validated the clinical applicability of open-loop control using a dual-threshold control system based on harmonic component spectral integration but noted limitations in noise immunity. Addressing this, Kamimura et al. [46] proposed a relative power spectrum analysis method in 2019, distinguishing stable cavitation dose (SCD) from inertial cavitation dose (ICD) based on baseline spectral calibration, automatically stopping sonication upon reaching preset SCD or detecting ICD. In 2021, Robin et al. [47] innovatively developed a dynamic control strategy based on cumulative cavitation dose (CCD). Under fixed pressure conditions, baseline signals are pre-acquired, and real-time cavitation dose is decomposed into stable (integral of 3rd-9th harmonic energy) and inertial components. Sonication terminates when the normalized CCD reaches a preset threshold (CCDtarget).

Both studies achieved consistent BBB opening while effectively reducing the risk of tissue damage from oversonication by precisely quantifying MB dynamics (Table 1). However, open-loop systems carry a risk of pressure overshooting due to threshold-triggering mechanisms and cannot adapt to dynamic changes in MB concentration within the blood flow.

Closed-Loop Feedback Control Strategies Addressing the limitations of open-loop control spurred the development of closed-loop feedback control. Its core concept involves continuously monitoring MB cavitation signals (e.g., harmonics, subharmonics, ultraharmonics, broadband noise) to dynamically adjust ultrasound parameters (primarily PNP) for safe and effective BBB modulation. In 2017, Sun et al. [48] first reported a dual-channel adaptive controller, innovatively utilizing a proportional-integral algorithm to track subharmonic energy and broadband noise simultaneously. When subharmonic intensity reached a preset threshold, the system immediately terminated sonication and adjusted subsequent pulse PNP with a fixed step size (ΔPt) to suppress potential IC damage, achieving a preliminary balance between BBB opening efficacy and tissue protection.

The following year, Bing et al. [49] introduced area under the curve (AUC) to quantify sub/ultraharmonic amplitudes for enhanced signal stability. Their feedback algorithm compared the average AUC of three consecutive samples to a target threshold (AUCtarg), setting a dead zone (ε = 0.2 × AUCtarg) to filter noise. If the average AUC was within AUCtarg ± ε, pressure remained unchanged; otherwise, it was increased or decreased in 0.01-0.03 MPa steps. This cycle continued until sonication ended. The study further validated the algorithm's universality for various commercial MBs. In 2019, Çavuşoğlu et al. [46] developed a rapid pre-calibration technique, pre-mapping the cavitation activity zone for individual animals and dynamically adjusting subsequent pulse PNP based on real-time measured ICD value relative to the target zone boundaries. This method reduced spectral identification time from 30 minutes to 80 seconds, significantly improving efficiency, though potential red blood cell extravasation risk was observed. McDannold's team [50] proposed an efficient trigger-pressure-reduction strategy to enhance response speed and safety in 2020. In rat models, the system monitored 1.5 f_0 and 2.5 f_0 harmonic amplitudes in real-time; if any signal exceeded an ultra-high statistical threshold (baseline mean + 10 standard deviations), the current PNP was immediately halved and maintained until sonication ended. This method optimized BBB opening while minimizing overpressure risk but lacked consideration for baseline cavitation level variations between individuals. Addressing this, Chien et al. (2022) [51] proposed a "virtual pre-scan" method, establishing individualized SC baselines by calculating the sum of fourth harmonic signal magnitudes and setting a target cavitation level (TCL) accordingly. A closed-loop algorithm dynamically adjusted PNP to maintain SC levels within the TCL ± tolerance range while strictly monitoring IC events (terminating sonication upon exceeding threshold). The study identified 0.5-2 dB as a safe window in mouse models; increasing TCL to 1 dB enlarged BBB opening volume by 14-fold while exceeding 3 dB significantly increased tissue damage risk. This approach was subsequently validated in large animal (pig) models [52]. Concurrently, Lee et al. [53] developed a control strategy based on a hyperbolic tangent model of pressure amplitude, regulating SC intensity using third harmonic integration. Sonication automatically terminated upon a 20% intensity drop. It immediately reduced pressure upon detecting broadband noise indicative of IC, effectively preventing tissue damage overshoot and demonstrating good bio-adaptive control advantages in a glioblastoma mouse model (Table 1).

Other Monitoring Strategies Lv's team [54] pio-

Table 1 Research Basis Information for Cavitation Monitoring Controllers

Study	Model	Ultrasound parameters	Focus area	Microbubble	Monitoring target	Control type	Sonication termination
O'reilly (2012)	Rats	Frequency: 551.5 kHz RPF: 2 Hz Pulse duration: 10 ms Total treatment time: 2 min	The top of the cranium	Denity 0.02 mL/kg^{-1}	1.5f_0 and 2.5f_0 ultraharmonics	Open-loop	Stop with ultraharmonics
Tsai (2016)	Rats	dual-frequency FUS transducer: 0.55 MHz and 1.1 MHz Pulse duration: 10 ms PRF = 1 Hz Total treatment time: 90 s power range: 2-7 W	The top of the cranium	SonoVue 0.1 ml/kg^{-1}	Subharmonics dose (threshold method)	Open-loop	Sub-harmonics dose reached 0.55 MHz
Huang (2017)	Pigs	Frequency: 230 kHz RPF: 2 Hz Total sonication time: 50 s Power range: 3-10 W	The porcine brain	Denity 4 ml/kg^{-1}	Spectral integration of the subharmonic (threshold method)	Open-loop	Dual-Threshold Consecutive Trigger
Kamimur (2019)	Monkeys	Frequency: 500 kHz PRF: 5 Hz Pulse length: 10 ms Total treatment time: 2 min	Targe1: Hippocampus Target 2: 2 cm caudal offset Target 3: 2 cm rostral offset	SonoVue 0.3 ml/kg^{-1}	The SCD and ICD (threshold method)	Open-loop	End of duration
Sun (2017)	Rats	Frequency: 274.3 kHz PRF: 1 Hz/4 Hz Pulse duration: 32.3 ms	Striatum and hippocampus.	Optison 300 μl/kg^{-1}	harmonic emission (HE) and broadband emission (BE)	Open-loop	Detected BE/HE threshold reached
Robin (2021)	Mice	Frequency: 1.5 MHz PRF: 2 Hz Pulse length: 10 ms	The left striatum	Definity 0.1 μL/g^{-1}	the 3rd to 9th harmonic frequencies.	Open-loop	Reach the preset target value
Bing (2018)	Rats	Frequency: 0.5 MHz PRF: 1 Hz Pulse length: 10 ms Total treatment time: 125 s	Hippocampus on both sides	Optison: 30 μl/kg^{-1} Denity: 6 μl/kg^{-1} Nanobubble: 737 μl/kg^{-1}	AUC by summing at sub- or ultra- harmonics amplitudes within ± 0.05 MHz bandwidth	Real-time closed-loop	End of duration
Çavuşoğlu (2019)	Mice	frequency: 650 KHz PRF: 1 Hz Pulse duration: 10 ms Total treatment time: 5 min	The top of the cranium	BG8235 1.1-1.2 μl/kg^{-1}	the broadband response	Real-time closed-loop	End of duration
McDannol (2020)	Rats	Frequency: 660 kHz PRF: 1.1 Hz Pulse duration: 5 ms Power range: 0.16-0.39 W Total treatment time: 55 s	Most of the right hemisphere of the brain	Denity: 20 μl/kg^{-1} BG8774: 20 μl/kg^{-1} MSB4: 20 μl/kg^{-1}	subharmonic and bandwidth	Real-time closed-loop	End of duration
Chien (2022)	Mice	Frequency: 1.5 MHz| Pulse length: 6.7 ms	The brainstem	Denity 8 × 10^8 Mbs/ml	SC level: sum spectrum magnitude at the third harmonic IC level: sum spectrum magnitude at 3.3 ± 0.02 MHz	Real-time closed-loop	End of duration
Chien (2022)	Pigs	Frequency: 2.25 MHz PRF: 1 Hz Pulse length: 10 ms Total treatment time: 180 s	The cortical brain region	Denity 10 μl/kg^{-1}	SC level: sum spectrum magnitude at the fourth harmonic IC level: sum spectrum magnitude at 2.1 ± 0.02 MHz	Real-time closed-loop	End of duration
Lee (2022)	Mice	Frequency: 1.64 MHz PRF: 1 Hz Pulse length: 10 ms	The entire tumor and its periphery	Denity/10 μl/kg^{-1}	The third harmonic level	Real-time closed-loop	End of duration

neered a novel ultrasound imaging monitoring mode alongside acoustic control techniques. Using support vector machines for ultrasound image detection, they achieved cavitation region classification (accuracy > 0.9). Improved watershed algorithms yielded a cavitation extraction Dice coefficient of 93.69%, and sparse array full-focus imaging enhanced computational efficiency by 40%. The team's successful tracking of cavitation evolution was demonstrated in bovine liver and human tissue phantom experiments.

Conclusion and Perspective

FUS-MBs technology achieves reversible BBB opening primarily through cavitation effects, with safety critically dependent on precise control of acoustic parameters, microbubbles properties, and skull acoustics. SC is the dominant mechanism, while IC correlates with tissue damage, underscoring the necessity for precise cavitation intensity management in clinical applications. The progression from open-loop to closed-loop feedback control strategies has substantially improved regulation precision, enabling real-time discrimination of cavitation types through spectral analysis of harmonic and broadband noise emissions. Despite significant advancements, key challenges persist. The mechanisms driving heterogeneous ultrasound responses across different brain regions remain unclear, and deeper investigation is required into the dynamic distribution of microbubbles within blood flow and their interactions with endothelial cells. Furthermore, systematic evaluation is needed regarding the potential long-term effects of repeated BBB opening and determining optimal treatment intervals. Future research priorities include achieving precise control under multimodal imaging guidance, developing intelligent parameter optimization algorithms, and conducting large-scale clinical validation to facilitate comprehensive clinical translation of this technology.

Acknowledgment

Not applicable.

Authors' Contributions

Na Li conceived and designed the review, performed the literature search, and drafted the manuscript. Fan Li contributed to the literature search and selection, and critically revised the manuscript for important intellectual content. Both authors read and approved the final manuscript and agree to be accountable for all aspects of the work.

Funding

This work was supported by the National Natural Science Foundation of China (Grant No. 82272012), the Shanghai Chest Hospital Science and Technology Development Fund, and the Key Science-Technology Project of Songjiang District Committee on Science and Technology (Grant No. 2023SJKWGG042)

Data Availability

Not applicable.

Declarations

Ethics approval and consent to participate

Not applicable.

Conflict of interest

The authors have no conflict of interest to declare.

Consent for publication

Not applicable.

References

[1] Knox EG, Aburto MR, Clarke G, Cryan JF, O'Driscoll CM. The blood-brain barrier in aging and neurodegeneration. Mol Psychiatry 2022;27:2659-2673.

[2] Zhao Z, Nelson AR, Betsholtz C, Zlokovic BV. Establishment and dysfunction of the blood-brain barrier. Cell 2015;163:1064-1078.

[3] Zhao P, Wu T, Tian Y, You J, Cui X. Recent advances of focused ultrasound induced blood-brain barrier opening for clinical applications of neurodegenerative diseases. Adv Drug Deliv Rev 2024;209:115323.

[4] Keiser MS, Chen YH, Davidson BL. Techniques for intracranial stereotaxic injections of adeno-associated viral vectors in adult mice. Curr Protoc Mouse Biol 2018;8:e57.

[5] D'Amico RS, Aghi MK, Vogelbaum MA, Bruce JN. Convection-enhanced drug delivery for glioblastoma: a review. J Neurooncol 2021;151:415-427.

[6] Tan JS, Jaffar Ali MNB, Gan BK, Tan WS. Next-generation viral nanoparticles for targeted delivery of therapeutics: Fundamentals, methods, biomedical applications, and challenges. Expert Opin Drug Deliv 2023;20:955-978.

[7] Saksena J, Hamilton AE, Gilbert RJ, Zuidema JM. Nanomaterial payload delivery to central nervous system glia for neural protection and repair. Front Cell Neurosci 2023;17:1266019.

[8] Rao R, Patel A, Hanchate K, Robinson E, Edwards A, Shah S, et al. Advances in focused ultrasound for the treatment of brain tumors. Tomography 2023;9:1094-1109.

[9] Liu HL, Yang HW, Hua MY, Wei KC. Enhanced therapeutic agent delivery through magnetic resonance imaging-monitored focused ultrasound blood-brain barrier disruption for brain tumor treatment: an overview of the current preclinical status. Neurosurg Focus 2012;32:E4.

[10] Memari E, Khan D, Alkins R, Helfield B. Focused ultrasound-assisted delivery of immunomodulating agents in brain cancer. J Control Release 2024;367:283-299.

[11] Schoen S Jr, Kilinc MS, Lee H, Guo Y, Degertekin FL, Woodworth GF, et al. Towards controlled drug delivery in brain tumors with microbubble-enhanced focused ultrasound. Adv Drug Deliv Rev 2022;180:114043.

[12] Scott K, Klaus SP. Focused ultrasound therapy for Alzheimer's disease: exploring the potential for targeted amyloid disaggregation. Front Neurol 2024;15:1426075.
[13] Rezai AR, Ranjan M, Haut MW, Carpenter J, D'Haese PF, Mehta RI, et al. Focused ultrasound-mediated blood-brain barrier opening in Alzheimer's disease: long-term safety, imaging, and cognitive outcomes. J Neurosurg 2022;139:275-283.
[14] Jahangiri S, Yu F. Fundamentals and applications of focused ultrasound-assisted cancer immune checkpoint inhibition for solid tumors. Pharmaceutics 2024;16:411.
[15] Gorick CM, Breza VR, Nowak KM, Cheng VWT, Fisher DG, Debski AC, et al. Applications of focused ultrasound-mediated blood-brain barrier opening. Adv Drug Deliv Rev 2022;191:114583.
[16] Hughes A, Khan DS, Alkins R. Current and emerging systems for focused ultrasound-mediated blood-brain barrier opening. Ultrasound Med Biol 2023;49:1479-1490.
[17] Mondou P, Mériaux S, Nageotte F, Vappou J, Novell A, Larrat B. State of the art on microbubble cavitation monitoring and feedback control for blood-brain-barrier opening using focused ultrasound. Phys Med Biol 2023;68.
[18] Ching-Hsiang Fan, Chih-Kuang Yeh. Microbubble-enhanced focused ultrasound-induced blood–brain barrier opening for local and transient drug delivery in central nervous system disease. Journal of Medical Ultrasound 2014;22:183-193.
[19] McDannold N, Vykhodtseva N, Hynynen K. Targeted disruption of the blood-brain barrier with focused ultrasound: association with cavitation activity. Phys Med Biol 2006;51:793-807.
[20] Apfel RE, Holland CK. Gauging the likelihood of cavitation from short-pulse, low-duty cycle diagnostic ultrasound. Ultrasound Med Biol 1991;17:179-185.
[21] Bader KB, Holland CK. Gauging the likelihood of stable cavitation from ultrasound contrast agents. Phys Med Biol 2013;58:127-144.
[22] Jin Q, Kang ST, Chang YC, Zheng H, Yeh CK. Inertial cavitation initiated by polytetrafluoroethylene nanoparticles under pulsed ultrasound stimulation. Ultrason Sonochem 2016;32:1-7.
[23] Chen H, Kreider W, Brayman AA, Bailey MR, Matula TJ. Blood vessel deformations on microsecond time scales by ultrasonic cavitation. Phys Rev Lett 2011;106:034301.
[24] Tung YS, Marquet F, Teichert T, Ferrera V, Konofagou EE. Feasibility of noninvasive cavitation-guided blood-brain barrier opening using focused ultrasound and microbubbles in nonhuman primates. Appl Phys Lett 2011;98:163704.
[25] Rigollet S, Rome C, Ador T, Dumont E, Pichon C, Delalande A, et al. FUS-mediated BBB opening leads to transient perfusion decrease and inflammation without acute or chronic brain lesion. Theranostics 2024;14:4147-4160.
[26] Gao Y, Gao S, Zhao B, Zhao Y, Hua X, Tan K, et al. Vascular effects of microbubble-enhanced, pulsed, focused ultrasound on liver blood perfusion. Ultrasound Med Biol 2012;38:91-98.
[27] Izhar M, Thakur A, Park DJ, Chang SD. Ultrasound mediated blood-brain barrier opening increases brain tumor biomarkers: A review of preclinical and clinical trials. J Liq Biopsy 2024;6:100277.
[28] Jung O, Thomas A, Burks SR, Dustin ML, Frank JA, Ferrer M, et al. Neuroinflammation associated with ultrasound-mediated permeabilization of the blood-brain barrier. Trends Neurosci 2022;45:459-470.
[29] Chen M, Peng C, Wu H, Huang CC, Kim T, Traylor Z, et al. Numerical and experimental evaluation of low-intensity transcranial focused ultrasound wave propagation using human skulls for brain neuromodulation. Med Phys 2023;50:38-49.
[30] Gerstenmayer M, Fellah B, Magnin R, Selingue E, Larrat B. Acoustic transmission factor through the rat skull as a function of body mass, frequency and position. Ultrasound Med Biol 2018;44:2336-2344.
[31] Fletcher SP, Zhang Y, Chisholm A, Martinez S, McDannold N. The impact of pulse repetition frequency on microbubble activity and drug delivery during focused ultrasound-mediated blood-brain barrier opening. Phys Med Biol 2024;69.
[32] Carpentier A, Stupp R, Sonabend AM, Dufour H, Chinot O, Mathon B, Ducray F, Guyotat J, Baize N, Menei P, de Groot J, Weinberg JS, Liu BP, Guemas E, Desseaux C, Schmitt C, Bouchoux G, Canney M, Idbaih A. Repeated blood-brain barrier opening with a nine-emitter implantable ultrasound device in combination with carboplatin in recurrent glioblastoma: a phase I/II clinical trial. Nat Commun 2024;15:1650.
[33] Wasielewska JM, White AR. "Focused ultrasound-mediated drug delivery in humans - a path towards translation in neurodegenerative diseases". Pharm Res 2022;39:427-439.
[34] Olumolade OO, Wang S, Samiotaki G, Konofagou EE. Longitudinal motor and behavioral assessment of blood-brain barrier opening with transcranial focused ultrasound. Ultrasound Med Biol 2016;42:2270-2282.
[35] Shin J, Kong C, Cho JS, Lee J, Koh CS, Yoon MS, et al. Focused ultrasound-mediated noninvasive blood-brain barrier modulation: preclinical examination of efficacy and safety in various sonication parameters. Neurosurg Focus 2018;44:E15.
[36] Parks TV, Szuzupak D, Choi SH, Alikaya A, Mou Y, Silva AC, et al. Noninvasive disruption of the blood-brain barrier in the marmoset monkey. Commun Biol 2023;6:806.
[37] Martinez PJ, Song JJ, Castillo JI, DeSisto J, Song KH, Green AL, et al. Effect of microbubble size, composition, and multiple sonication points on sterile inflammatory response in focused ultrasound-mediated blood-brain barrier opening. ACS Biomater Sci Eng 2024;10:7451-7465.
[38] O'Reilly MA, Huang Y, Hynynen K. The impact of standing wave effects on transcranial focused ultrasound disruption of the blood-brain barrier in a rat model. Phys Med Biol 2010;55:5251-5267.
[39] Choi JJ, Feshitan JA, Baseri B, Wang S, Tung YS, Borden MA, et al. Microbubble-size dependence of focused ultrasound-induced blood-brain barrier opening in mice in vivo. IEEE Trans Biomed Eng 2010;57:145-154.
[40] Arvanitis CD, Livingstone MS, Vykhodtseva N, McDannold N. Controlled ultrasound-induced blood-brain barrier disruption using passive acoustic emissions monitoring. PLoS One 2012;7:e45783.
[41] de Jong N, Emmer M, van Wamel A, Versluis M. Ultrasonic characterization of ultrasound contrast agents. Med Biol Eng Comput 2009;47:861-873.
[42] Pouliopoulos AN, Kwon N, Jensen G, Meaney A, Niimi Y, Burgess MT, et al. Safety evaluation of a clinical focused ultrasound system for neuronavigation guided blood-brain barrier opening in non-human primates. Sci Rep 2021;11:15043.
[43] O'Reilly MA, Hynynen K. Blood-brain barrier: real-time feedback-controlled focused ultrasound disruption by using an acoustic emissions-based controller. Radiology 2012;263:96-106.
[44] Tsai CH, Zhang JW, Liao YY, Liu HL. Real-time monitoring of focused ultrasound blood-brain barrier opening via subharmonic acoustic emission detection: implementation of confocal dual-frequency piezoelectric transducers. Phys Med Biol 2016;61:2926-2946.
[45] Huang Y, Alkins R, Schwartz ML, Hynynen K. Opening the blood-brain barrier with mr imaging-guided focused ultrasound: preclinical testing on a trans-human skull porcine model. Radiology

2017;282:123-130.

[46] Kamimura HA, Flament J, Valette J, Cafarelli A, Aron Badin R, Hantraye P, et al. Feedback control of microbubble cavitation for ultrasound-mediated blood-brain barrier disruption in non-human primates under magnetic resonance guidance. J Cereb Blood Flow Metab 2019;39:1191-1203.

[47] Ji R, Karakatsani ME, Burgess M, Smith M, Murillo MF, Konofagou EE. Cavitation-modulated inflammatory response following focused ultrasound blood-brain barrier opening. J Control Release 2021;337:458-471.

[48] Sun T, Zhang Y, Power C, Alexander PM, Sutton JT, Aryal M, et al. Closed-loop control of targeted ultrasound drug delivery across the blood-brain/tumor barriers in a rat glioma model. Proc Natl Acad Sci U S A 2017;114:E10281-E10290.

[49] Bing C, Hong Y, Hernandez C, Rich M, Cheng B, Munaweera I, et al. Characterization of different bubble formulations for blood-brain barrier opening using a focused ultrasound system with acoustic feedback control. Sci Rep 2018;8:7986.

[50] McMahon D, Lassus A, Gaud E, Jeannot V, Hynynen K. Microbubble formulation influences inflammatory response to focused ultrasound exposure in the brain. Sci Rep 2020;10:21534.

[51] Chien CY, Yang Y, Gong Y, Yue Y, Chen H. Blood-brain barrier opening by individualized closed-loop feedback control of focused ultrasound. BME Front 2022;2022:9867230.

[52] Chien CY, Xu L, Pacia CP, Yue Y, Chen H. Blood-brain barrier opening in a large animal model using closed-loop microbubble cavitation-based feedback control of focused ultrasound sonication. Sci Rep 2022;12:16147.

[53] Lee H, Guo Y, Ross JL, Schoen S Jr, Degertekin FL, Arvanitis C. Spatially targeted brain cancer immunotherapy with closed-loop controlled focused ultrasound and immune checkpoint blockade. Sci Adv 2022;8:eadd2288.

[54] Shijie Lv, Huifeng Zheng, Runguang Yao, Yuebin Wang, Baoming Peng. Monitoring acoustic cavitation effects in tissues under the action of HIFU based on ultrasound images. Applied Acoustics 2024;219:109937.